Global Change Biology (1998) **4,** 505–521

Potentially complex biosphere responses to transient global warming

RONALD P. NEILSON[1] and RAYMOND J. DRAPEK[2]
[1]*USDA Forest Service, Forestry Sciences Laboratory, 3200 SW Jefferson Way, Corvallis, OR 97331, USA,* [2]*Department of Forest Science, Oregon State University, Corvallis, OR 97331, USA*

Abstract

Feedback interactions between terrestrial vegetation and climate could alter predictions of the responses of both systems to a doubling of atmospheric CO_2. Most previous analyses of biosphere responses to global warming have used output from equilibrium simulations of current and future climate, as compared to more recently available transient GCM simulations. We compared the vegetation responses to these two different classes of GCM simulation (equilibrium and transient) using an equilibrium vegetation distribution model, MAPSS. Average climatologies were extracted from the transient GCM simulations for current and doubled (2×) CO_2 concentrations (taken to be 2070–2099) for use by the equilibrium vegetation model. However, the 2 × CO_2 climates extracted from the transient GCM simulations were not in equilibrium, having attained only about 65% of their eventual 2 × CO_2 equilibrium temperature change. Most of the differences in global vegetation response appeared to be related to a very different simulated change in the pole to tropic temperature gradient. Also, the transient scenarios produced much larger increases of precipitation in temperate latitudes, commensurate with a minimum in the latitudinal temperature change. Thus, the (equilibrium) global vegetation response, under the transient scenarios, tends more to a greening than a decline in vegetation density, as often previously simulated. It may be that much of the world could become greener during the early phases of global warming, only to reverse in later, more equilibrial stages. However, whether or not the world's vegetation experiences large drought-induced declines or perhaps large vegetation expansions in early stages could be determined by the degree to which elevated CO_2 will actually benefit natural vegetation, an issue still under debate. There may occur oscillations, perhaps on long timescales, between greener and drier phases, due to different frequency responses of the coupled ocean–atmosphere–biosphere interactions. Such oscillations would likely, of themselves, impart further reverberations to the coupled Earth System.

Keywords: general vegetation model, global warming, land surface, terrestrial biosphere, transient

Introduction

The prospect of global warming due to human influences has galvanized the research community into making future projections of both climatic change and ecosystem impacts from climatic change. However, ecosystem and climate modellers have long recognized that each system is influenced by the other through a variety of energy and mass transfer feedbacks. Atmosphere–ocean feedbacks are also of critical importance in determining potential future climates. Dynamic coupling of all three systems, plus the cryosphere, is a primary goal of Earth System Modelling. Scientific advancement toward this goal has progressed through a series of stages. At the time of the First Assessment Report (FAR) of the IPCC (Intergovernmental Panel on Climate Change), scenarios of future climate were being produced by Atmospheric General Circulation Models (AGCM), using prescribed ocean and land-surface properties and run to equilibrium, producing an 'average' climatology for both current (1 × CO_2) and the equivalent of doubled CO_2 (2 × CO_2) radiative forcing (Cubasch & Cess 1990). By the Second Assessment Report (SAR), the AGCMs had been coupled to Oceanic General Circulation Models (AOGCM) and were being used to simulate timeseries of historic and projected future changes in the concentrations of greenhouse gases with a prescribed, static land surface (Gates

Correspondence: Ronald P. Neilson, fax +1/541-750-7329, e-mail neilson@fsl.orst.edu

et al. 1996). The development of Dynamic General Vegetation Models (DGVM), designed to replace the static land surface models, has lagged behind that of the AOGCMs and is only now being realized (Woodward *et al.* 1995; Foley *et al.* 1996; Neilson & Running 1996). Even though the transient AOGCM scenarios were published in the SAR, the ecological impacts from working group II of the SAR were produced using the older FAR scenarios. The significant technological advances between the FAR and SAR scenarios beg the question of whether or not the terrestrial biosphere might respond quite differently than earlier projections based on the FAR scenarios. The purpose of this paper is to explore, using an equilibrium vegetation distribution model, some of the implications of and differences between the FAR and SAR scenarios with respect to potential vegetation responses to global warming. Some inferences of the possible dynamic responses of vegetation and biosphere–atmosphere feedbacks during transient global warming will be discussed.

Previous investigations of biosphere–atmosphere feedbacks have progressed on two separate fronts: (i) engineering of complex biophysical Soil–Vegetation–Atmosphere–Transfer schemes (SVAT) within the context of GCMs; and (ii) development of complex General Vegetation Models (GVM), independent of the GCMs. The former approach has been focused largely on the accuracy of biophysical simulation of mass and energy exchanges between the land surface and the atmosphere and can incorporate quite complex plant physiology, but little by way of ecological dynamics (Seth *et al.* 1994; Sellers *et al.* 1995; Sellers *et al.* 1997). The latter has focused less on biophysics and more on ecological processes with increasing emphasis on plant physiology, biogeochemistry and vegetation structure and distribution (VEMAP members 1995).

Global vegetation modelling for investigations of global warming impacts and feedbacks has progressed from empirical, correlational modelling, such as Holdridge (1947) to increasingly process-based equilibrium modelling of potential natural vegetation (e.g. VEMAP members 1995) to the first generation of DGVMs, which are only now emerging (Woodward *et al.* 1995; Foley *et al.* 1996; Neilson & Running 1996; Cramer, pers. comm.). Estimations of biosphere–atmosphere feedbacks have often involved coarse manipulations of the static vegetation maps within SVAT/GCMs, for example, removal of forests over the Amazonian or Boreal regions and comparing equilibrium differences (Dickinson & Henderson-Sellers 1988; Bonan *et al.* 1992; Henderson-Sellers *et al.* 1993; Eltahir & Bras 1994; Foley *et al.* 1994; Bonan *et al.* 1995; Kutzbach *et al.* 1996; Zeng *et al.* 1996). Alternatively, equilibrium vegetation models have been coupled iteratively to GCMs to explore changes in surface properties on regional and global climates (e.g. Claussen 1994; Betts *et al.* 1997). Roughness length, albedo and leaf area index (LAI) are among the most sensitive surface parameters affecting the climate (Henderson-Sellers 1992; Bonan *et al.* 1992; Foley *et al.* 1994; Claussen 1994; Bonan *et al.* 1995), but trace gas fluxes could be even more important (Henderson-Sellers 1994). The importance of ecosystem physiology was nicely demonstrated by manipulating photosynthesis and stomatal responses within a SVAT, while retaining a fixed vegetation structure (e.g. distribution and LAI; Sellers *et al.* 1997). In addition, the importance of dynamic vegetation structure (LAI) in concert with the physiological processes was demonstrated by iteratively coupling an equilibrium vegetation model with a GCM (Betts *et al.* 1997). Attempts have been made to estimate the transient carbon flux responses of vegetation to climate change by inferring the ecological changes that could occur between two equilibrium potential vegetation distributions, i.e. comparisons between vegetation maps from $1 \times CO_2$ and $2 \times CO_2$ simulations. These transient inferences have focused on the processes of vegetation dieback and establishment, primarily of forests, as they tend to shift from one location to another. Large lags between establishment and regrowth processes compared to dieback processes could produce a large pulse of CO_2 to the atmosphere, potentially acting as a positive feedback to global warming (Overpeck *et al.* 1990; King & Neilson 1992; Smith & Shugart 1993).

The conclusion from these studies is that, indeed, the feedbacks between the atmosphere and the biosphere could have profound influences on both systems and that the nature of the feedbacks span the full range of processes from complex biophysics to physiological, structural and ecological processes. However, most of the previous analyses were done using equilibrium GCM simulations with prescribed oceans. Dynamic feedbacks between the atmosphere and fully dynamic oceans play a critical role in atmospheric processes and in the context of transient AOGCMs could produce very different biosphere responses and hence biosphere–atmosphere feedbacks. Since the newer SAR scenarios are coupled to a dynamic ocean and since they are fully transient, they are clearly not in equilibrium at the time of $2 \times CO_2$ equivalent forcing, having only attained about 50–80% of their eventual equilibrium global temperature change (Kattenberg *et al.* 1996). Dynamic oceans in an AOGCM add considerable thermal inertia, as well as an oceanic mechanism for horizontal advection of large amounts of energy between latitudes. We examine the biogeographical changes predicted by the MAPSS model under global warming, focusing on the projected changes in surface-atmosphere feedback properties, implications for the transient carbon pulse hypothesis and uncertainties with respect to direct, physiological effects of elevated CO_2. This study is intended to explore vegetation responses

under two of the newer SAR GCM scenarios, compared to the older FAR scenarios and to examine some of the possible biosphere responses and uncertainties with respect to global warming and their implications for feedbacks to climate change. Although MAPSS is an equilibrium vegetation distribution model, it allows physiological adjustment to elevated CO_2 via changes in stomatal conductance as well as structural changes through LAI and vegetation distribution.

Methods

The MAPSS equilibrium biogeography model (Mapped Atmosphere–Plant–Soil System) operates under the assumption that maximum leaf area index (LAI, area of leaves per unit ground area) is constrained either by the availability of water for transpiration or by the availability of energy for growth. Energy constraints are simply imposed in the model on a biome basis; whereas, water balance constraints are directly calculated through a set of interacting nonlinear processes (Neilson 1995). Woody and grass life forms compete for both light and water while maintaining a site water balance consistent with observed runoff (Neilson & Marks 1994; Neilson 1995). Through iteration, LAI is maximized to a level that just utilizes the available soil moisture during the growing season. A three layer soil hydrology model allows competition between grasses and woody plants in the upper soil layer, where water is apportioned to the two life forms as a function of the product of their respective LAIs and stomatal conductances. Woody plants also have access to the second soil layer. A third soil layer is required for accurate simulation of base flow and to constrain percolation of water from the upper layers. Stomatal conductance is modulated by atmospheric vapour pressure deficit and soil water potential. The MAPSS model also contains a physiologically conceived rule-base, which determines leaf form (broadleaf, needleleaf) and phenology (evergreen, deciduous; timing of leaf on and leaf off) for the woody vegetation. These lifeform characteristics are combined with model output of overstory and understory LAI and thermal tolerances to assign a vegetation classification, largely at the biome level, but extending to lower physiognomic levels in some cases. There are currently 47 unique vegetation classes simulated by the model (not shown). Surface feedback properties, such as albedo and surface roughness values were assigned to all MAPSS vegetation classes, an aggregated summary of which is presented in Table 1.

Global simulations were on a 0.5° lat./long. grid (Leemans & Cramer 1991; Neilson 1993; Neilson & Marks 1994). Simulations over the conterminous U.S. were on a 10 km, equal-area Albers projection (Neilson 1995). Two sets of $2 \times CO_2$ climate scenarios were used as input for this analysis: equilibrium models featured in the First Assessment Report (FAR) of the Intergovernmental Panel on Climate Change (Cubasch & Cess 1990) and transient models that have been included in the Second Assessment Report (SAR, Gates *et al.* 1996). The FAR GCMs included in this analysis were from the Geophysical Fluid Dynamics Laboratory (GFDL R30, Manabe *et al.* 1990; Wetherald *et al.* 1990), Oregon State University (OSU, Schlesinger & Zhao 1989), the United Kingdom Meteorological Office (UKMO, Wilson & Mitchell 1987), and the Goddard Institute of Space Studies (GISS, Hansen *et al.* 1988). The FAR GCM global $2 \times CO_2$ temperature changes ranged from 2.8 °C (OSU) to 5.2 °C (UKMO) and precipitation increases ranged from 8% (OSU) to 15% (UKMO) (Cubasch & Cess 1990) (Table 2). The two SAR scenarios included in this analysis (HADCM2GHG, HADCM2SUL) were derived from the Hadley Center transient GCM simulations (Mitchell *et al.* 1995; Johns *et al.* 1997). The global $2 \times CO_2$ temperature sensitivity (temperature change at equilibrium) of the SAR scenarios ranged from 2.5 to 2.7 °C, but the models had only attained a temperature increase of 1.7 °C at the time of CO_2 doubling (Kattenberg *et al.* 1996) (Table 2). Global $2 \times CO_2$ precipitation increases were not reported for the SAR scenarios (Kattenberg *et al.* 1996)

The SAR scenarios differ in several important ways from the equilibrium scenarios. The SAR GCMs are coupled to a fully dynamic, 3D ocean, as opposed to a simple, prescribed ocean. The FAR scenarios were equilibrium; while, the SAR simulations were transient, being forced by observed changes in greenhouse gases from about 1800 to the present and then into the future using IPCC projections of future greenhouse gas emissions. Since MAPSS is not yet able to simulate transient climates, a control period (1961–90) and a $2 \times CO_2$ climate

Table 1 Aggregated MAPSS vegetation classes, number of MAPSS classes found in the aggregated class, and the range of albedo and roughness values across the aggregated classes

Aggregated MAPSS Class	#MAPSS classes	Albedo	Roughness length (m)
Tundra	1	0.16	0.07
Taiga/Tundra	1	0.12	0.50
Boreal Conifer Forest	1	0.12	1.00
Temperate Evergreen Forest	3	0.12	1.00
Temperate Mixed Forest	4	0.13–0.17	1.00
Tropical Broadleaf Forest	1	0.12	2.60
Savanna/Woodland	11	0.12–0.19	0.55–1.00
Shrub/Woodland	9	0.14–0.27	0.07–0.12
Grassland	9	0.20–0.25	0.07
Arid Land	6	0.17–0.33	0.01–0.10
Ice	1	0.80	0.01

Table 2 GCM simulated changes in temperature and precipitation aggregated over the world (land and oceans), the world land area, and over the conterminous U.S. FAR (First Assessment Report) scenarios are: OSU, GISS, GFDL-R30, UKMO. SAR (Second Assessment Report) scenarios are: HADCM2GHG, HADCM2SUL (see text for further explanation).

	World Total		World Land Area[1]		Conterminous USA	
	ΔT (C°)	ΔP (%)	ΔT (C°)	ΔP (%)	ΔT (C°)	ΔP (%)
OSU	2.8	8	3	20.9	3	2.1
GISS	4.2	11	4.3	16	4.4	5.1
GFDL-R30	4	8	3.9	18.7	4.2	18.9
UKMO	5.2	15	6	15.1	6.6	11.3
HADCM2GHG	1.7	NR	4.3	3.2	3.7	30.7
HADCM2SUL	1.7	NR	3.5	1.7	2.8	22.9

[1]Excluding Antarctica; NR , Not Reported

period (2070–2099) were selected and compared as with the equilibrium scenarios. However, at the time of $2 \times CO_2$ radiative forcing, the simulations had attained only about 64–68% of the eventual equilibrium temperature change, due to thermal lags in the oceans. Scenarios were applied by calculating deltas of climate variables between the $1 \times$ and $2 \times CO_2$ simulations and applying the deltas back to the observed baseline climate. Precipitation and humidity deltas were calculated as ratios and temperature deltas were calculated as differences. Two Hadley scenarios were examined, one without sulphate aerosol forcing (HADCM2GHG) and one with aerosol forcing (HADCM2SUL). The $2 \times CO_2$ global temperature sensitivity at equilibrium for all SAR scenarios discussed by Kattenberg *et al.* (1996) ranged from 2.1 to 4.6 °C; while the warming at the time of CO_2 doubling ranged from 1.3 to 3.8 °C. Therefore, the two Hadley scenarios discussed here produced relatively modest warming compared to the other SAR scenarios.

All land surface parameters were averaged (area weighted) across the globe and zonally for 10° intervals of latitude and were compared between simulations under current and future climates. Global AET/PPT ratios were calculated by first area-weighting the actual evapotranspiration (AET) and precipitation (PPT) and calculating the ratio directly from the global averages, rather than area-weighting the ratios *per se*. The two approaches are not equivalent, but give similar trends. The climate change scenarios were also summarized for the U.S. to demonstrate the magnitude of some regional deviations from global averages. Global areas for each of four forest types (boreal conifer, temperate evergreen, temperate mixed, and tropical broadleaf) were calculated from MAPSS output for control and GCM scenarios. Areas changing from nonforest to these four forest types and *vice versa* were calculated for each GCM (vs. the control).

Elevated CO_2 affects the physiology of plants, possibly increasing productivity, nitrogen-use-efficiency and water-use-efficiency (reduced transpiration per carbon fixed), conferring some drought resistance (Bazzaz *et al.* 1996; Kirschbaum 1996). However, natural forests may not experience as much direct CO_2 benefit as observed in growth chambers or with young plants (McGuire *et al.* 1995; Bazzaz *et al.* 1996). Water-use-efficiency (WUE) may be increased by elevated CO_2, but decreased by elevated temperature (Bazzaz *et al.* 1996). Increased air temperatures and reduced transpiration would cause leaf temperatures to increase, either causing leaf damage or requiring increased transpiration for leaf cooling (Bazzaz *et al.* 1996). Also, over time species may adapt to elevated CO_2 and down regulate photosynthesis (Körner 1995; Bazzaz *et al.* 1996; Sellers *et al.* 1996). Early growth increases may disappear as the system approaches carrying capacity limited by water or nutrients (Körner 1995). Shifts in species composition will likely result from different sensitivities to elevated CO_2 (Körner 1995; Bazzaz *et al.* 1996). Direct CO_2 effects may diminish at higher CO_2 levels, while temperatures continue to increase (Körner 1995; Bazzaz *et al.* 1996). Doubled CO_2-induced changes in water-use-efficiency (WUE) are emulated in MAPSS through a 35% reduction in maximum stomatal conductance (Eamus 1991). Although elevated CO_2 can also enhance productivity, those processes are not included in the equilibrium version of MAPSS. The rate of productivity will determine how rapidly vegetation approaches a carrying capacity, but should have little effect on the carrying capacity, per se. MAPSS specifically simulates the biophysically constrained carrying capacity of the vegetation by maximizing LAI. Internal feedbacks within MAPSS produce increased LAI if stomatal conductance is reduced under elevated CO_2. The simulated increase in LAI may indicate a true biophysical constraint on increased productivity. Since the direct CO_2 effect in MAPSS is only imparted to stomatal conductance, we refer to this process as the 'WUE' effect. The MAPSS model was run with and without the increase in WUE

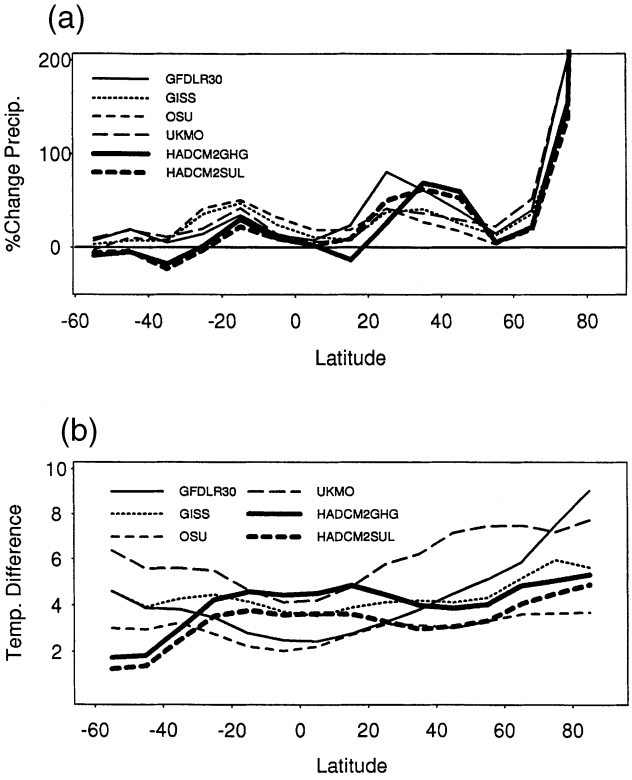

Fig. 1 Area-weighted average changes in (a) precipitation (%) (by 10° latitudinal intervals) and (b) temperature (°C) for each FAR (light lines) and SAR (heavy lines) scenario.

in order to bracket the potential ecosystem response to elevated CO_2 concentration.

Results

The FAR and SAR scenarios have distinctly different qualitative properties (Table 2, Fig. 1). The SAR scenarios are distinctly cooler over the entire world (land and oceans) than are the FAR scenarios. However, over just the world's land area the SAR scenarios exhibit about the same temperature increase as do the FAR scenarios (Table 2). Interestingly, the two SAR scenarios produced much less precipitation increase over the world's land area (1.7–3.2%, excluding Antarctica) than do the FAR scenarios (15–21%), but considerably more precipitation increase over the conterminous USA (Table 2). The reason for the increase over the USA is apparent from the latitudinal profiles of temperature and precipitation change (Fig. 1). The FAR scenarios show generally increasing temperature deltas with increasing latitude; however, the SAR scenarios show much higher tropical temperatures and are more subdued in their temperature increase with latitude. The SAR scenarios exhibit a minimum temperature increase at about 40–50° N latitude, commensurate with the largest increases in precipitation (Fig. 1). The SAR scenarios show the least temperature increase over the southern latitudes, south of about 40°, in contrast to the FAR scenarios which show a maximum increase at both north and south high latitudes. The GISS FAR scenario is intermediate with an almost flat temperature response with latitude (Fig. 1), being hotter in the tropics than most FAR scenarios and cooler at the higher latitudes.

The precipitation changes are also markedly different between the FAR and SAR scenarios. The FAR scenarios show relatively large precipitation increases in tropical and subtropical to temperate latitudes; whereas, the SAR scenarios show much less tropical rainfall increase and much more temperate latitude increase, as is apparent over the conterminous USA(Table 2, Fig. 1). Even though the two SAR scenarios are from only a single GCM, they are still unique compared to all four of the FAR scenarios.

The vegetation response to the SAR scenarios was also quite different from that of the FAR scenarios, but the response was strongly modulated by the direct CO_2 effect on water-use-efficiency. Increased water-use-efficiency (WUE) under the control climate, produces increases in forest area, LAI, surface roughness, and runoff (Tables 3, 4). In the same simulation, decreases occurred in albedo and AET values, and the ratio of AET to precipitation (AET/PPT). Under control climate, a 35% reduction in stomatal conductance (high-WUE effect) only produced a 3% reduction in AET, due largely to a 20% increase in LAI. If the system were strictly linear, a 35% reduction in stomatal conductance and a 20% increase in LAI would be expected to result in a 22% reduction in AET [1–(1.2 $\times$ 0.65) = 0.22]. That only a 3% reduction in AET was simulated, attests to the curvilinearity of system responses and the tendency for stomatal conductance and LAI changes to cancel each other in the simulated system.

With increased WUE, all climate scenarios produced increases in global forest area (Table 3). Without increased WUE, all scenarios produced decreases in forest area, though the decreases were relatively modest for the SAR scenarios (3–27% loss), compared to the FAR scenarios (5–73% loss).

Control forest area exhibited two peaks with latitude, at 55° N and at 5° S (Fig. 2). Increases in global forest area for FAR high-WUE scenarios occurred largely north of 50° N latitude (Figs 2b, 3b). Tropical forests also contributed substantially to the FAR high-WUE forest area increases though the percentage change of forest area in the tropics was not as high as in other latitudes. Some of the FAR high-WUE scenarios produced decreases in forest area in the temperate latitudes below 50° N. The FAR normal-WUE scenarios produced consistent decreases for all latitudes below 50° N and consistent increases at high northern latitudes. The latitudinal patterns of change in forest area for SAR high-WUE scenarios

Table 3 Global area ($km^2 \times 10^6$) of each major forest biome under current and future climates (4 FAR, 2 SAR scenarios).

	Baseline		FAR GCMs		SAR GCMs	
	Normal WUE	High WUE	Normal WUE	High WUE	Normal WUE	High WUE
Boreal Conifer	10.2	11.4	3.5–12.6	9.8–13.6	11.0–11.1	11.6–11.8
Temp. Evergreen	11.4	15.1	2.4–9.3	11.8–15.9	10.6–11.0	14.8–15.4
Temp. Mixed	7.4	7.8	2.5–8.0	9.3–12.0	10.1–10.7	10.3–11.1
Trop. Broadleaf	14.1	22.9	3.3–11.1	14.6–24.0	9.8–10.1	19.1–19.5
Total Forest	43.1	57.2	11.7–41.0	49.5–59.4	31.4–42.0	56.6–57.0

FAR, First Assessment Report; SAR, Second Assessment Report. WUE, Water-use-efficiency; Normal, $1xCO_2$; High, $2xCO_2$ concentration

Table 4 Global area weighted average values for LAI, surface roughness, albedo, AET, runoff, precipitation, and AET/precipitation. These values are calculated for 4 First Assessment Report (FAR) GCMs and for the 2 Second Assessment Report (SAR) GCMs and for MAPSS runs where the water use efficiency (WUE) is increased through a 35% reduction in maximum stomatal conductance. Due to rounding errors of area-weighted calculations, sums may not be precise.

	Baseline		FAR GCMs		SAR GCMs	
	Normal WUE	High WUE	Normal WUE	High WUE	Normal WUE	High WUE
LAI ($m^2\ m^{-2}$)	4.9	5.9	2.2–4.7	5.2–6.0	4.8	5.8
Roughness (m)	0.73	0.88	0.45–0.72	0.81–0.91	0.68–0.69	0.85
Albedo	0.18	0.17	0.18–0.20	0.16–0.17	0.17–0.18	0.16–0.17
AET (mm)	480	457	528–571	508–547	531–545	507–521
Runoff (mm)	294	318	339–425	360–447	267	293
PPT (mm)	794	794	914–961	914–961	807–820	807–820
AET/PPT (mm)	0.62	0.59	0.55–0.63	0.53–0.60	0.67	0.63–0.64

LAI is all-sided. AET, Actual Evapotranspiration; PPT, Precipitation

were similar to those produced by some FAR high-WUE scenarios, except that peak levels were not as high (Figs 2c, 3c). Similarly, the latitudinal pattern of changes in forest area for the SAR normal-WUE scenarios was similar to the FAR normal-WUE scenarios, though the decreases occurring across all latitudes south of 55° N were not as large as those from the most severe FAR scenarios.

Gains in forest area in temperate and boreal regions under both FAR and SAR scenarios resulted mostly from conversions of the cold nonforest types (tundra and taiga/tundra, Table 5). Without the assumption of increased WUE, large areas of forest in the temperate latitudes are lost to nonforest for both FAR and SAR scenarios, although the magnitude is much higher under FAR (Fig. 2). Under the high-WUE scenarios, forest gains largely outweigh the forest losses (both FAR and SAR, Figs 2, 3, 4).

Changes in global averages of LAI were consistent with the changes in forest area and distribution (Tables 3, 4, 5) with increases for high-WUE scenarios and decreases for the normal-WUE scenarios. The normal-WUE decreases in LAI were more pronounced for the FAR scenarios. Control zonal mean LAI values were maximal at the tropics and in the north and south temperate regions (Fig. 5a). The increases in global mean LAI values for high-WUE scenarios were greatest in high northern latitudes under both the FAR and SAR scenarios (Figs 5b, 5c, 6, 7). LAI also increased over the northern-most latitudes even when increased WUE was not assumed, but these increases were offset by decreases through the lower latitudes. LAI decreases were much less pronounced for the SAR scenarios than they were for the FAR scenarios (Figs 5b, 5c, 6, 7). However, both SAR scenarios produced slight declines in tropical forest LAI, even with increased WUE, in contrast to the FAR scenarios, which generally produced increases in both tropical forest area and LAI, excepting the hottest FAR scenario, UKMO (Figs 6, 7).

Simulated decreases in LAI are generally due to a drought-induced decline, primarily caused by higher temperatures and increased evaporative demand. There tend to be strong regional patterns of both increased LAI and decreased LAI; however, there are very few locations showing no change in LAI under any scenario (Figs 6, 7). Among all the GCMs, the area within the major forest biomes that is simulated to undergo a drought-induced LAI decline tends to increase with the simulated global average temperature increase (Fig. 8). An interesting

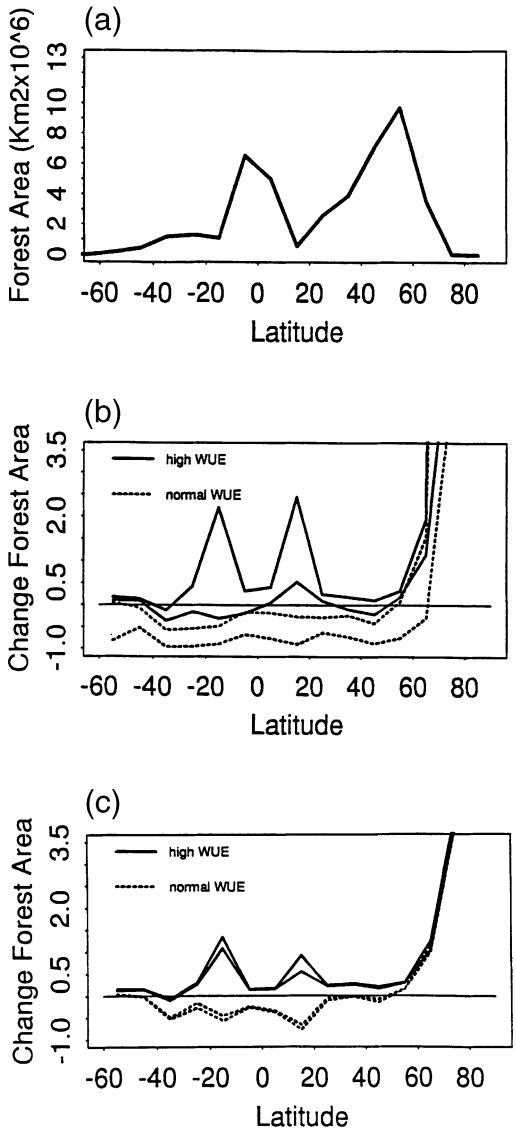

Fig. 2 Forest area ($km^2 \times 10^6$) by 10E latitudinal intervals. (a) control climate, (b) minimum and maximum proportional change for First Assessment Report (FAR) GCMs with high water use efficiency (WUE, solid lines) and with normal-WUE (dashed lines), (c) minimum and maximum proportional change for Second Assessment Report (SAR) GCMs with high water use efficiency (WUE) and with normal-WUE.

exception is the LAI response under the GISS FAR scenario. The areas within different forest biomes of both dieback and vegetation increase under the GISS scenario are more similar to forest responses under the cooler SAR scenarios (HADCM2) than they are to the FAR scenarios. Examination of the zonal temperature and precipitation changes (Fig. 1) indicates that the GISS scenario is more similar to the SAR scenarios in latitudinal temperature patterns, while being about the same as the FAR scenarios with respect to precipitation changes. The different character of the zonal temperature curves between the FAR and SAR scenarios appears to modulate a very different response from the vegetation with much more forest dieback under the FAR scenarios. If, due to its unique latitudinal temperature change profile (Fig. 1), the GISS scenario is considered an outlier, the trends in Fig. 8 are quite striking.

There are also remarkable similarities in the vegetation responses across all scenarios, both FAR and SAR. The LAI changes in the southern hemisphere, especially South America, are very similar with respect to relative regional patterns among all the scenarios (Fig. 6). For example, the eastern Amazon experiences drought-induced decline in all three scenarios in Fig. 6; while, adjacent savannas experience increased growth in all three scenarios. More regionally detailed patterns also emerge in central South America under all scenarios. Similar parallels among the scenarios are evident in Africa where all three scenarios produced increased vegetation growth in sub-Saharan regions. South of the Sahara are banded regions of vegetation decline or increased vegetation growth leading into the Congo which either exhibit little change or some decline in all scenarios. Southern Africa and Madagascar also exhibit similar patterns of change in all scenarios. Examination of the more detailed output over the U.S. (Fig. 7) reveals a similar parallelism. For example, the South-west and central Texas regions appear to be wetter (greener) in all three simulations. These regional patterns appear to be driven by prevailing regional stormtrack and vegetation patterns (Wendland & Bryson 1981). One exception is the eastern U.S. in the HADCM2SUL simulation, which has a strong regional sulphate aerosol forcing minimizing the warming in that area.

Over the conterminous USA the relationship between forest decline and average simulated temperature changes breaks down due to large increases in simulated precipitation, primarily within the SAR scenarios (Table 2). Precipitation increases over the conterminous U.S. range from 23 to 31% under the SAR scenarios and only from 2 to 19% under the FAR scenarios. Yet, the two SAR scenarios produce among the lowest increases in temperature over the USA (Table 2). The vegetation responses to the SAR scenarios over the conterminous U.S. are generally of considerably increased density (LAI) compared to those under the FAR scenarios (Figs 6, 7).

Global and zonal averages for surface roughness and albedo changes were generally consistent with the changes simulated for LAI and forest area, with only minor exceptions (Figs 9, 10; Tables 3, 4, 5). Whether the surface parameters increase or decrease depends primarily on the inclusion or not of the direct CO_2 effect (high-WUE). Simulated AET values also increased globally for all scenarios. Normal-WUE scenarios produced higher AET values than the high-WUE scenarios,

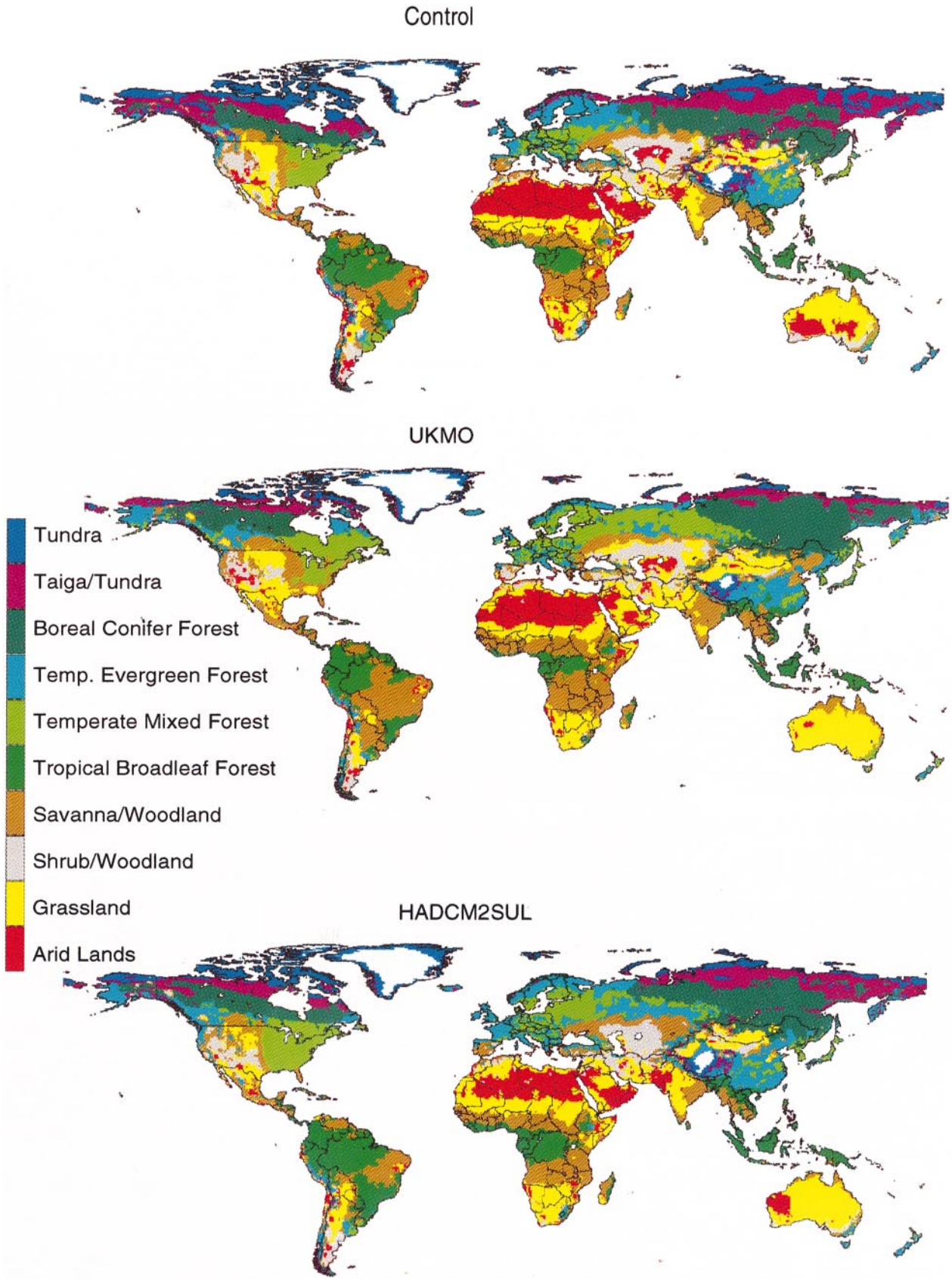

Fig. 3 MAPSS simulated global vegetation distribution: (a) control climate, (b) UKMO (FAR scenario) with high-WUE, (c) HADCM2SUL (SAR scenario) with high-WUE.

Table 5 Ranges in areas (in $km^2 \times 10^6$) undergoing changes in biome types are calculated for MAPSS model runs with and without CO_2 effects for 4 FAR and 2 SAR scenarios.

Biome Change	FAR GCMs		SAR GCMs	
	Normal WUE	High WUE	Normal WUE	High WUE
Cold Non-forest to T/B Forest	4.1–6.0	7.7–11.9	7.0–8.0	7.2–8.5
Non-forest to T/B Forest	0.0–0.0	0.3–1.9	0.2–0.3	2.2–2.6
Non-Forest to Tropical Forest	0.0–0.0	2.1–8.9	0.0–0.0	4.3–4.5
T/B Forest to Non-forest	14.2–24.7	0.9–5.1	3.7–4.4	0.5–0.9
Tropical Forest to Non-Forest	7.6–10.9	0.0–3.0	4.7–4.8	0.2–0.3

'Cold Non-forest' refers to the 'tundra' and 'taiga/tundra' vegetation classes; 'T/B Forest' refers to all temperate and boreal forest classes; 'Non-forest' refers to the 'savanna/woodland', 'shrub/woodland', 'grassland', and 'arid land' vegetation classes; and 'Tropical Forest' refers to the 'tropical broadleaf forest' vegetation class (Table 1)

but the normal-WUE FAR scenarios produced particularly high AET values. Runoff increased for all FAR scenarios, but decreased slightly for the SAR normal-WUE scenarios, being essentially unchanged for the SAR high-WUE simulations. The proportion of precipitation being transpired (AET/PPT) changed less than 7% under all scenarios; while, LAI varied from a loss of 55% under the most extreme normal-WUE FAR scenario to a gain of 22% under the least extreme high-WUE FAR scenario. The feedback between CO_2-induced change in stomatal conductance and LAI change appears to nearly stabilize the global ratio of AET/PPT.

The vegetation responses to global warming exhibit interesting properties with respect to spatial scale. The GCMs produce changes in temperature and precipitation fields at relatively coarse scales, on the order of several degrees of latitude and longitude (i.e. hundreds of kilometres), consistent with large-scale circulation patterns. Generally, the deltas of temperature and precipitation vary smoothly over geography reflecting large-scale shifts in the general circulation regime. These large-scale changes are interpolated to higher resolution grids for application to the observed climate, which has been interpolated from station data to the higher resolution grid. Therefore, if different patterns of change, perhaps even of opposite sign, arise in adjacent cells of the higher resolution grid, then the response to the coarse-grid changes in temperature and precipitation are in part a function of the background climate and vegetation, which vary more rapidly over the high resolution grid than do the GCM variables (see also Neilson & Marks 1994). Although this observation is apparent on the global grid, it is even more so on the 10 km USA grid (Figs 4, 6, 7). Upon close examination, it becomes apparent that certain areas are more prone to express the decline than other areas. For example, in Oregon (Figs 4, 6, 7), the areas that tend to exhibit a decline under the cooler scenarios (high-WUE) are the coldest, wettest areas along the coastline or in the high mountains. These are areas that are currently energy-limited, but shift to being water-limited under the warmer climate. Adjacent areas that are currently water-limited, actually increase in growth under the cooler scenarios, but then shift to a decline under the hotter scenarios. Other topographic features also stand out. For example, the central valley of California consistently exhibits an increased vegetation density (Figs 4, 6, 7); while, the surrounding mountains show either increases or decreases, depending on the scenario. Such local to regional contrasts in vegetation response would likely impart local feedbacks affecting local weather patterns (Pielke & Avissar 1990).

Discussion

Under all potential future climate scenarios, forests are projected to shift northward into currently nonforested areas. The drier boundaries of forests at temperate latitudes either expand into dry continental interiors or contract away from them, depending on whether the direct effects of elevated CO_2 are considered, and on whether the scenario is derived from the equilibrium GCM simulations (FAR) or from the transient simulations (SAR).

Large increases in LAI, with equilibrium vegetation conditions under all high-WUE scenarios, suggest that vegetation mass as a whole and global terrestrial carbon stocks would likely increase, acting as a negative feedback. However, potential increases in tropical forest area (FAR scenarios) and possibly even temperate forest area may be limited due to land-use considerations (Henderson-Sellers 1994). Though equilibrium vegetation models often produce predictions of increasing terrestrial carbon stocks in the long term (Neilson 1993), vegetation carbon stocks may actually decrease in the short term (Neilson *et al.* 1994). If rapid climate change produced large areas of forest die-back, imbalances between rates of carbon release and vegetation regrowth and migration could produce a large carbon pulse, acting as a positive feedback to global warming (King & Neilson 1992; Smith & Shugart 1993). However, only the earlier FAR scenarios without elevated WUE exhibit sufficient forest dieback to produce a carbon pulse of the magnitude simulated by King & Neilson (1992).

Even in regions that remain forested, a drop in LAI (surrogate for drought-induced decline or die back) could result in carbon releases from increased drought, pest

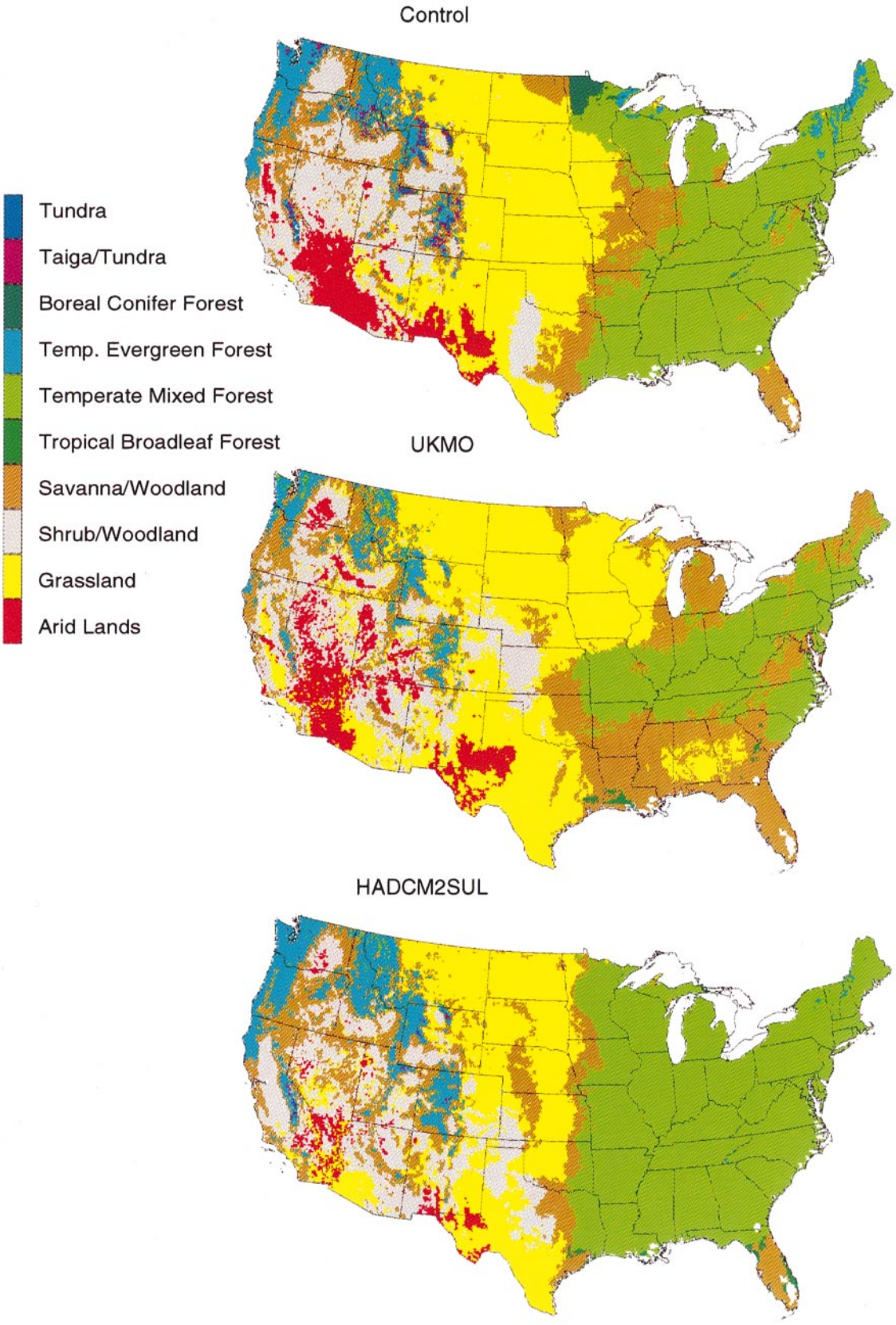

Fig. 4 MAPSS simulated conterminous USA vegetation distribution: (a) control climate, (b) UKMO (FAR scenario) with high-WUE, (c) HADCM2SUL (SAR scenario) with high-WUE.

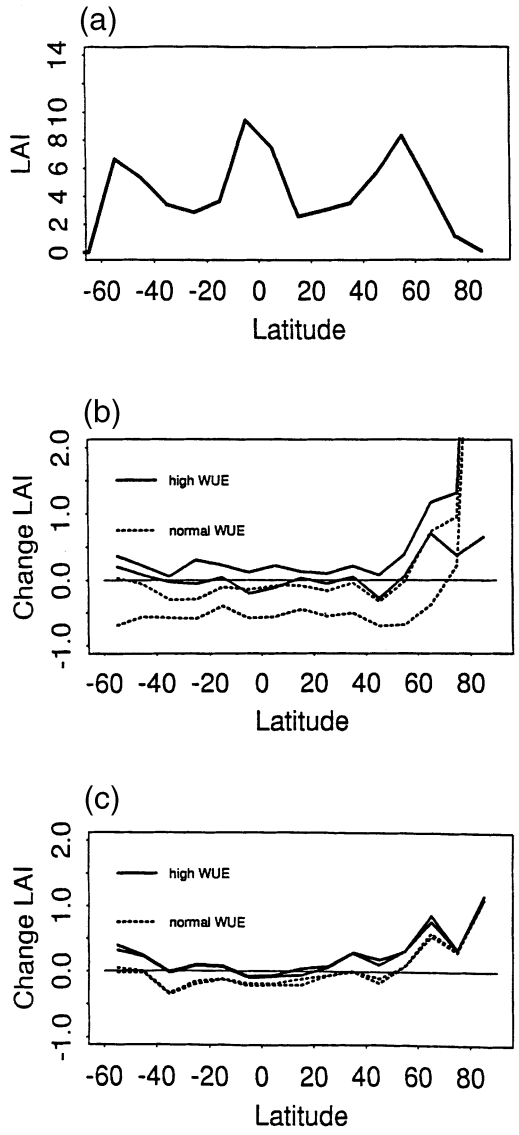

Fig. 5 Area-weighted average LAI by 10° latitudinal intervals. (a) control climate (b) minimum and maximum proportional change for FAR GCMs with high-WUE and with normal-WUE, (c) minimum and maximum proportional change for SAR GCMs with high-WUE and with normal-WUE.

infestations and catastrophic fire. The area of LAI decline in the FAR scenarios in temperate and boreal forests ranges from 24 to 86%, even with a CO_2 effect, an amount which may be sufficient to produce a substantial carbon pulse during transient forest adjustment to climate change. However, a similar magnitude of impact is only attained under the SAR scenarios without increased WUE, producing declines over 51–75% of the area of any given forest biome (Neilson *et al.* 1997). When a WUE effect is included under the SAR scenarios, the area of extra-tropical forest decline is limited to only 12–29% of any given forest type and is not likely sufficient to produce a substantial carbon pulse. Across all scenarios, Temperate Mixed Forests appear to be the most sensitive to forest decline and dieback as indicated by the percentage area of decreased LAI (Fig. 8). By far the largest natural distribution of this forest type is in eastern USA (Figs 3, 4, 7). Boreal Conifer Forests are the next most sensitive, followed by Temperate Evergreen and Tropical Broadleaf Forests, which exhibit similar levels of sensitivity (Fig. 8). However, under the SAR scenarios, the tropical forests exhibit a bit more sensitivity (Fig. 8).

The role of direct, physiological effects of elevated CO_2 is of particular concern in the analysis of feedbacks. We have seen that under the newer SAR scenarios, the world could experience a large enhancement of ecosystem productivity if the full benefits of elevated CO_2 are realized. However, if the impact of elevated CO_2 on natural ecosystems is considerably less than observed in growth chambers, then the world could experience significant declines in ecosystem biomass, resulting in a release of carbon and a positive feedback to global warming. The releases of carbon from declining ecosystems would likely be facilitated by large-scale disturbances, particularly drought, pests and fire. These disturbances could produce an overshoot in forest dieback, resulting in even more carbon releases thus enhancing positive feedbacks even further.

Increases in forest area are expected to be slow due to lags in dispersal and soil formation processes (Smith & Shugart 1993). Thus, whether a carbon pulse occurs or not may well depend on the strength and timing of the direct effects of elevated CO_2 concentration on forest water-use-efficiency. If the WUE effect is pronounced and appears relatively early in global warming, forests could expand both in area and density, sequestering carbon. However, if the WUE effect is not very strong, then forests could undergo substantial dieback, releasing large amounts of carbon. Under the high-WUE conditions, the earth system might self-regulate to a generally stable balance. However, if the biosphere responds with widespread dieback, particularly of forests, one might expect a net positive feedback from a large carbon pulse which could be a de-stabilizing force in the coupled atmosphere–biosphere system.

Associated changes in surface roughness and albedo would act in somewhat different ways from the carbon feedback. The northward expansion of forest area with attendant changes in albedo and increases in surface roughness could produce a warming feedback as hypothesized for the Holocene by Foley *et al.* (1994). Thus, there may be at least two opposing feedbacks, a negative feedback from carbon sequestration, and a positive feedback from increased albedo. The changes in roughness and AET would be expected to shift the heat balance from sensible to latent heat, thereby damping the heating,

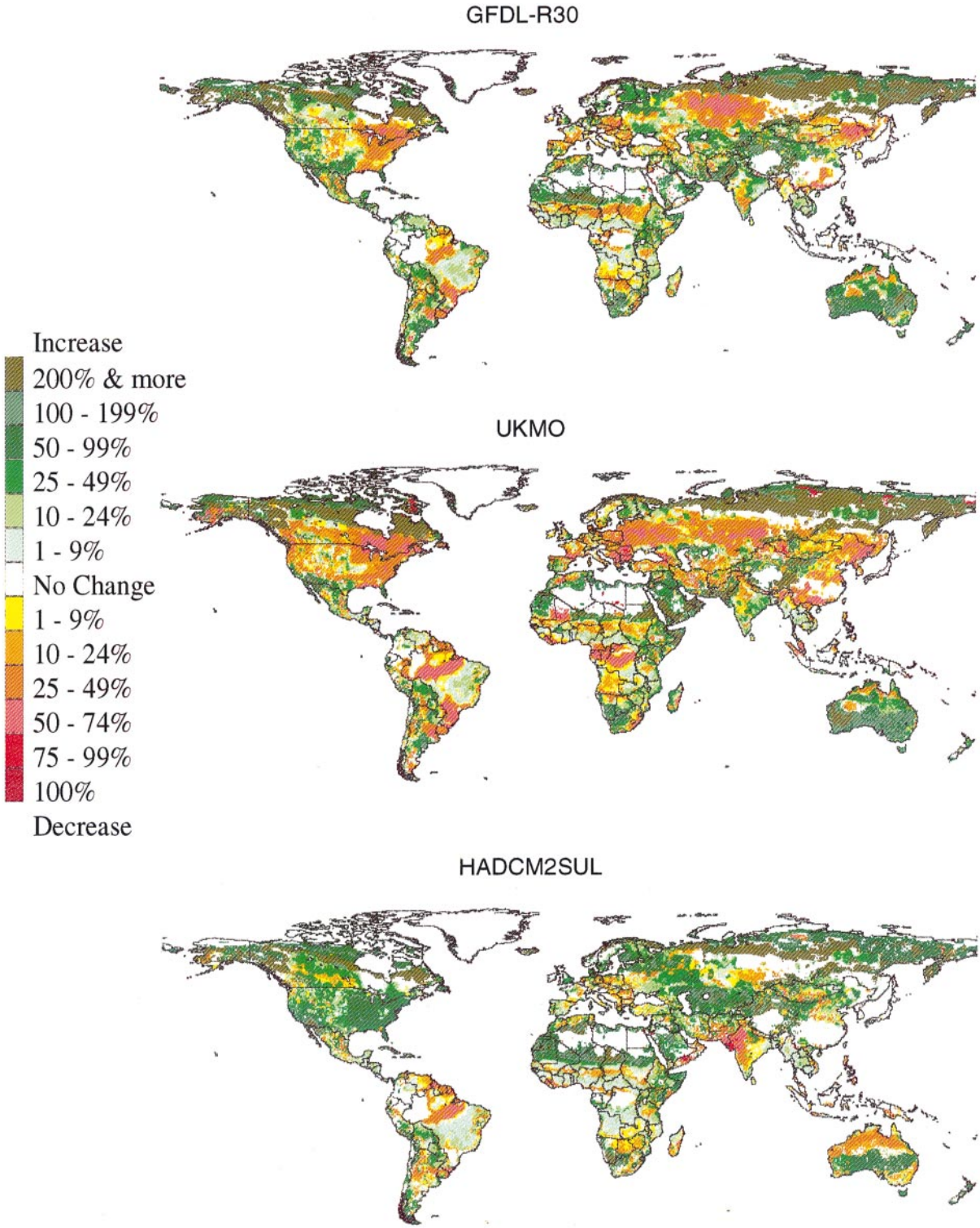

Fig. 6 MAPSS simulated percentage LAI changes over global land areas under two FAR scenarios (GFDL-R30, UKMO) and one SAR scenario (HADCM2SUL) with high water use efficiency (WUE).

a possible negative feedback. However, increased AET could form more clouds, which could either act as a warming blanket, or a cooling sunlight reflector, depending on cloud type and height (Washington 1992). Furthermore, the direct CO_2 effect can change the sign of the responses of vegetation from drought-induced

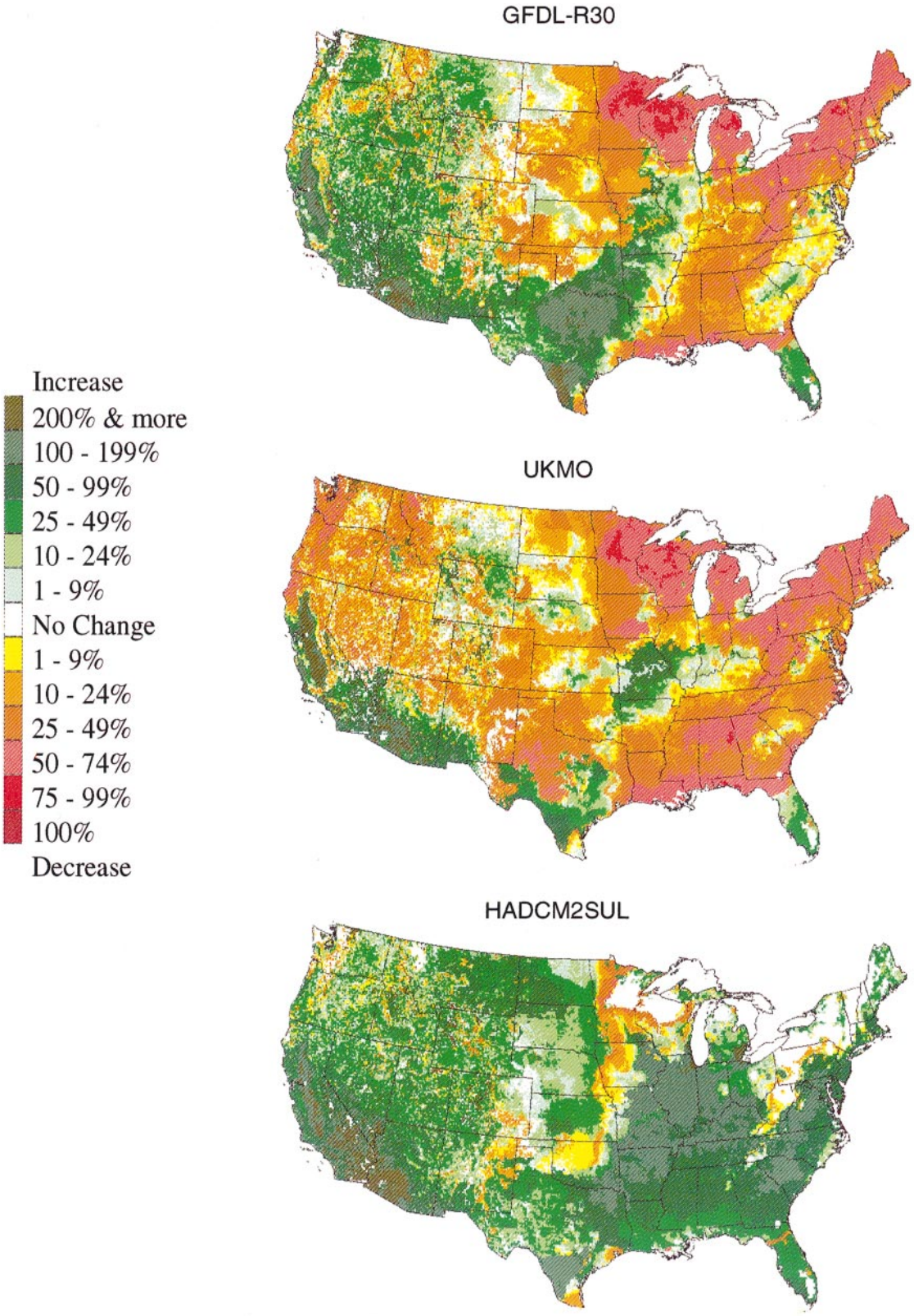

Fig. 7 MAPSS simulated percentage LAI changes over the conterminous USA under two FAR scenarios (GFDL-R30, UKMO) and one SAR scenario (HADCM2SUL) with high water use efficiency (WUE).

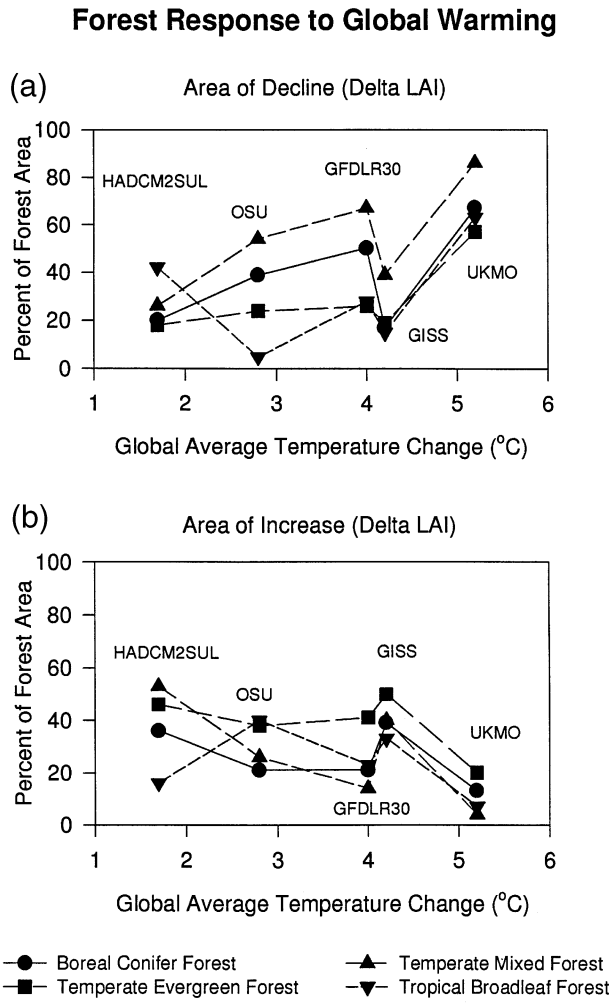

Fig. 8 The percentage area within major forest biomes which is simulated to undergo either a decline in LAI (a), or an increase in LAI (b) under one SAR (HADCM2SUL) and four FAR scenarios. The areas of decline or increase are plotted against the reported global average increase in temperature (land plus oceans) for each GCM. The two Hadley scenarios are sufficiently similar that only one is presented.

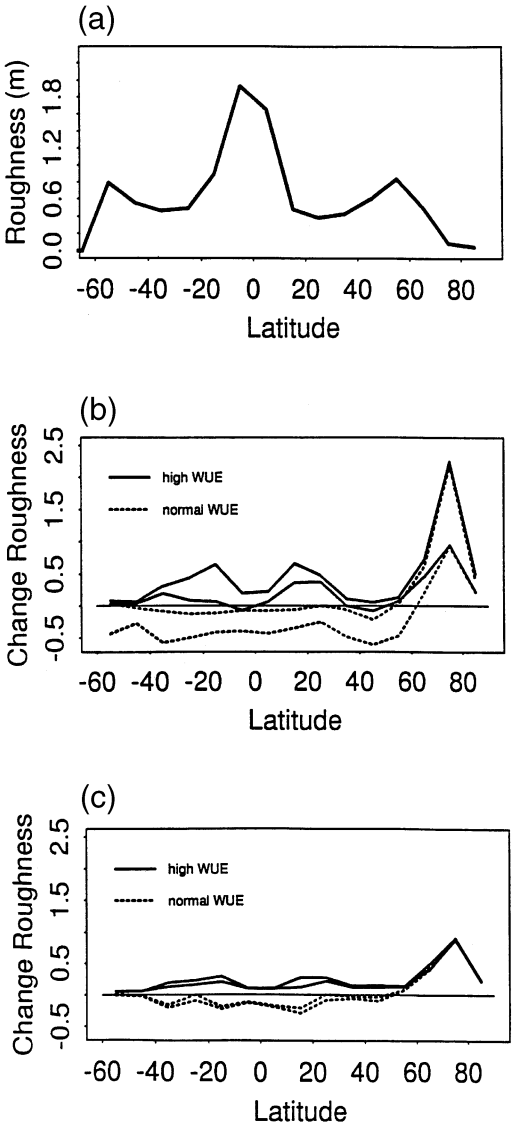

Fig. 9 Area-weighted average surface roughness (m) by 10° latitudinal intervals. (a) control climate (b) minimum and maximum proportional change for FAR GCMs with high-WUE and with normal-WUE, (c) minimum and maximum proportional change for SAR GCMs with high-WUE and with normal-WUE.

declines to extensive increases in growth. Thus, the CO_2 effect has the capability to modulate the sign of the response of all the primary feedback parameters.

It may be that in the early phases of global warming, while temperature increases are relatively small and CO_2 benefits are likely increasing, the world will experience increased vegetation biomass. However, in later stages of warming, temperatures and evaporative demand would continue to increase, while CO_2 benefits might begin tapering off. The global impact of increasing temperatures on declining forest area is evident when examined across all the scenarios (Fig. 8). However, the simulated relationship depicted in Fig. 8 includes the full benefit of $2 \times CO_2$ concentrations across all scenarios. One would expect that the relationship between forest dieback and global temperature change would be even stronger if the direct effects of CO_2 were gradually increased along with the temperature. Since the overall temperature sensitivity at equilibrium is similar between the FAR and SAR scenarios, the more deleterious FAR scenarios could be an accurate indication of the eventual biosphere response, after an initial greening period as simulated under the transient SAR scenarios. However, it is not clear whether or not the globe will ever approach climatic equilibrium within the next millennium, particularly if CO_2 concentrations were to approach 3 or 4 times current levels. Nor is it clear that a simulated equilibrium with a prescribed

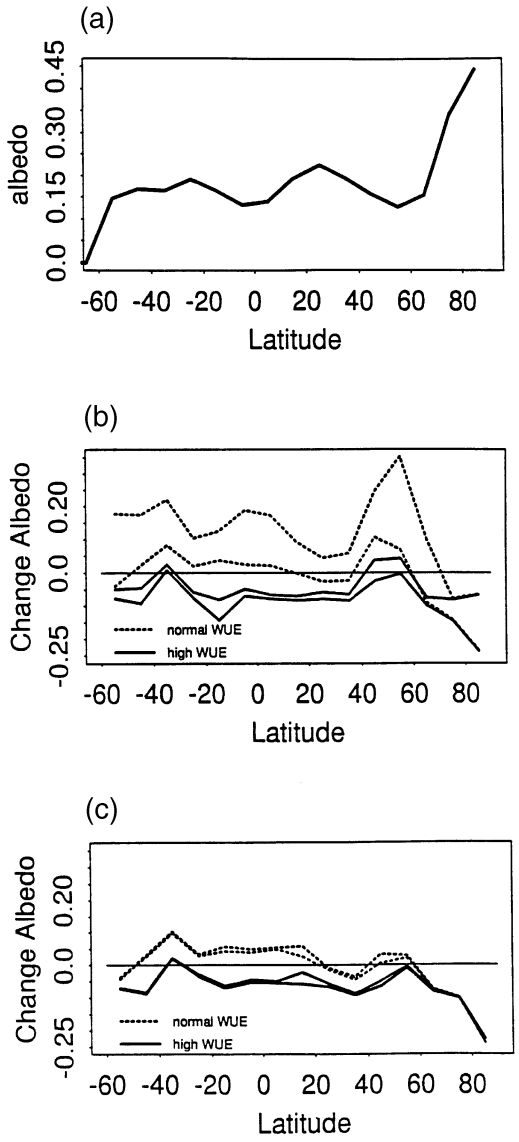

Fig. 10 Area-weighted average albedo by 10° latitude intervals. (a) control climate (b) minimum and maximum proportional change for FAR GCMs with high-WUE and with normal-WUE, (c) minimum and maximum proportional change for SAR GCMs with high-WUE and with normal-WUE.

ocean (FAR scenario) would be similar to an equilibrium simulation over a dynamic ocean, such as that in the SAR scenarios.

The SAR scenarios produce more mid- to high-latitude rainfall and less tropical rainfall than the FAR scenarios. This global shift in rainfall distribution, coupled with the very different latitudinal temperature shifts (Fig. 1) appears to ameliorate the mid- to high-latitude forest dieback; while, allowing some increased risk to tropical forest dieback. Thus, it may be that tropical forests could be most sensitive to transient shifts in climate and CO_2 in the early stages of warming; while, the risk might shift to the higher latitudes in the later stages of warming.

The results presented here leave us with the hypothesis that the biosphere's response to transient climate change could be very different from that simulated under equilibrium climates. Large areas of global forests could experience either dramatic dieback, or much improved growth, depending on the latitudinal pattern of temperature and precipitation changes, produced by the two classes of GCMs. If the equilibrium FAR simulations are a reasonable indication of the eventual equilibrium that might be reached by the SAR simulations, then the world could experience significant oscillations in vegetation response, from initially beneficial over large areas to potentially quite detrimental in later stages. Forests could go through a drought-induced decline in the tropics, with perhaps large releases of CO_2, in the early stages of global warming; while, temperate and high latitude forests experience increases in growth. However, if the global climate tends toward an equilibrium similar to the FAR scenarios in the later stages of global warming, the tropics might tend to recover, while the extratropical forests could come under drought stress.

Incorporating a dynamic ocean into a GCM appears to have profoundly affected the regional distribution of temperature and rainfall changes. The strong zonal and regional differences between the FAR and SAR scenarios are suggestive of a significant effect from a dynamic ocean, which alters the zonal energy distribution in the transient context. Significant oceanic advective energy transport could alter regional oceanic and land-surface temperature and rainfall patterns. Such shifts also can alter the flow structure of the atmosphere, perhaps modulating transitions between blocking meridional jetstream flow (N–S), or more zonal flow (W–E) (Weeks *et al.* 1997). The differences in the zonal temperature curves between the two classes of GCMs may be in part due to such large-scale differences in flow patterns, which in turn cause large regional differences in temperature and rainfall patterns over continents. Feedbacks among regions on continents and between the oceans and continents can serve to either re-enforce or diminish large-scale blocking patterns and hence regional climate regimes (Weeks *et al.* 1997).

Regional changes in land surface parameters are somewhat analogous to re-arranging the boulders in a stream. Airstream eddies and currents are shifted in often subtle ways. Changes in regional surface characteristics result in changes in regional pressure patterns, which in turn affect regional airstream patterns, storm tracks and regional weather. Thus, even if the global and zonal averages show little change under global warming, cumulative regional climate and vegetation changes could still produce large effects on global circulation patterns. The

regional changes in vegetation density under all the scenarios appear to have strong components of both local topographic and regional airmass/stormtrack forcing. These regionally forced changes in global circulation could further enhance or dampen regional land surface changes in a cascading sequence of complex feedback processes. Thus, inclusion of feedbacks within the ocean–atmosphere system could have a significant impact on simulations of the coupled vegetation–atmosphere responses to global warming.

Given that the biosphere also affects atmospheric circulation and regional to local latent and sensible heat exchanges, one can only speculate that incorporation of a dynamic biosphere will also impact global circulation patterns. Only a fully coupled Earth System Model, incorporating the atmosphere, oceans, cryosphere and biosphere in transient coupling will be able to accurately capture the potential feedbacks and possible consequences of global warming. However, the new results presented here, using an equilibrium vegetation model with the transient SAR and the equilibrium FAR scenarios, indicate some striking differences between the two sets of simulations. These results suggest hypotheses of vegetation change that could be much more complex than previously discussed and will depend on the relative timing of changes in CO_2, precipitation and temperature. Two substantial uncertainties are highlighted from these results: (i) how great will be the benefits of elevated CO_2 on vegetation physiology and what will be the timing of those benefits; and, (ii) how will the coupled ocean-atmosphere general circulation patterns and associated temperature and rainfall patterns evolve during transient dynamics toward eventual equilibrium conditions?

Acknowledgements

This research was supported by: the USDA Forest Service, PNW, NE and SE stations and the USGS/BRD (CA-1268-1-9014).

References

Bazzaz FA, Bassow SL, Berntson GM, Thomas SC (1996) Elevated CO_2 and terrestrial vegetation: implications for and beyond the global carbon budget. In: *Global Change and Terrestrial Ecosystems* (eds Walker B, Steffen W), pp. 43–76. Cambridge University Press, Cambridge.

Betts RA, Cox PM, Lee SE, Woodward FI (1997) Contrasting physiological and structural vegetation feedbacks in climate change simulations. *Nature*, **387,** 796–799.

Bonan GB, Chapin FS, Thompson SL (1995) Boreal forest and tundra ecosystems as components of the climate system. *Climatic Change*, **29,** 145–168.

Bonan GB, Pollard D, Thompson SL (1992) Effects of boreal forest vegetation on global climate. *Nature*, **359,** 716–718.

Claussen M (1994) On coupling global biome models with climate models. *Climate Research*, **4,** 203–221.

Cubasch U, Cess RD (1990) Processes and Modeling. In: *Climate Change: The IPCC Scientific Assessment* (eds Houghton JT, Jenkins GJ, Ephraums JJ), pp. 69–91. Cambridge University Press, Cambridge.

Dickinson RE, Henderson-Sellers A (1988) Modeling tropical deforestation: a study of GCM land-surface parameterizations. *Quarterly Journal of the Royal Meteorological Society,* **114,** 439–462.

Eamus D (1991) The interaction of rising CO_2 and temperatures with water use efficiency. *Plant, Cell and Environment*, **14,** 843–852.

Eltahir EAB Bras RL (1994) Sensitivity of regional climate to deforestation in the Amazon basin. *Advances in Water Resources*, **17,** 101–115.

Foley JA, Kutzbach JE, Coe MT, Levis S (1994) Feedbacks between climate and boreal forests during the Holocene epoch. *Nature*, **371,** 52–54.

Foley JA, Prentice IC, Ramankutty N, Levis S, Pollard D, Sitch S, Haxeltine A (1996) An integrated biosphere model of land surface processes, terrestrial carbon balance, and vegetation dynamics. *Global Biogeochemical Cycles*, **10,** 603–628.

Gates WL, Henderson-Sellers A, Boer GJ *et al.* (1996) Climate Models – Evaluation. In: *Climate Change 1995: the Science of Climate Change. Contribution of Working Group I to the Second Assessment Report of the Intergovernmental Panel of Climate Change* (eds Houghton JT, Meira Filho LG, Callander BA, Harris N, Kattenberg A, Maskell K), pp. 235–284. Cambridge University Press, Cambridge.

Hansen J, Fung I, Lacis A, Rind D, Lebedeff S, Ruedy R (1988) Global climate changes as forecast by Goddard Institute for Space Studies three-dimensional model. *Journal of Geophysical Research*, **93,** 9341–9364.

Henderson-Sellers A (1992) Assessing the sensitivity of land-surface scheme to parameters used in tropical-deforestation experiments. *Quarterly Journal of the Royal Meteorological Society,* **118,** 1101–1116.

Henderson-Sellers A (1994) Land-use change and climate. *Land Degradation and Rehabilitation*, **5,** 107–126.

Henderson-Sellers A, Dickinson RE, Durbridge TB, Kennedy PJ, McGuffie K, Pitman AJ (1993) Tropical deforestation: Modeling local to regional-scale climate change. *Journal Geophysical Research*, **98,** 7289–7315.

Holdridge LR (1947) Determination of world plant formations from simple climatic data. *Science*, **105,** 367–368.

Johns TC, Carnell RE, Crossley JF *et al.* (1997) The second Hadley Centre coupled ocean-atmosphere GCM: Model description, spinup and validation. *Climate Dynamics*, **13,** 103–134.

Kattenberg A, Giorgi F, Grassl H *et al.* (1996) Climate Models – Projections of Future Climate. In: *Climate Change 1995: the Science of Climate Change. Contribution of Working Group I to the Second Assessment Report of the Intergovernmental Panel on Climate Change* (eds Houghton JT, Meira Filho LG, Callander BA, Harris N, Kattenberg A, Maskell K), pp. 289–357. Cambridge University Press, Cambridge.

King GA, Neilson RP (1992) The transient response of vegetation to climate change: A potential source of CO_2 to the atmosphere. *Water, Air, and Soil Pollution*, **64,** 365–383.

Kirschbaum MUF (1996) Ecophysiological, Ecological, and Soil Processes in Terrestrial Ecosystems: A Primer on General Concepts and Relationships. In: *Climate Change 1995: Impacts, Adaptations and Mitigation of Climate Change: Scientific-Technical Analyses. Contribution of Working Group II of the Second Assessment Report of the Intergovernmental Panel on Climate Change* (eds Watson RT, Zinyowera MC, Moss RH), pp. 57–74. Cambridge University Press, Cambridge.

Körner C (1995) Towards a better experimental basis for up scaling plant responses to elevated CO_2 and climate warming. *Plant, Cell and Environment*, **18,** 1101–1110.

Kutzbach J, Bonan G, Foley J, Harrison SP (1996) Vegetation and soil feedbacks on the response of the African monsoon to orbital forcing in the early to middle Holocene. *Nature*, **384,** 623–626.

Leemans R, Cramer WP (1991) *The IIASA database for mean monthly values of temperature, precipitation, and cloudiness on the global terrestrial grid*. International Institute for Applied Systems Analysis RR-91–18, 1–62.

Manabe S, Wetherald RT, Mitchell JFB Meleshko V, Tokioka T (1990) Equilibrium climate change- and its implications for the future. In: *Climate change: the IPCC scientific assessment* (eds Houghton JT, Jenkins GJ, Ephraums JJ), pp. 131–172. Cambridge University Press, New York.

McGuire AD, Melillo JM, Joyce LA (1995) The role of nitrogen in the response of forest net primary production to elevated atmospheric carbon dioxide. *Annual Review of Ecology and Systematics*, **26,** 473–503.

Mitchell JFB Johns TC, Gregory JM, Tett S (1995) Climate response to increasing levels of greenhouse gases and sulphate aerosols. *Nature*, **376,** 501–504.

Neilson RP (1993) Vegetation redistribution: a possible biosphere source of CO_2 during climatic change. *Water, Air, and Soil Pollution*, **70,** 659–673.

Neilson RP (1995) A model for prediction continental-scale vegetation distribution and water balance. *Ecological Applications*, **5,** 362–385.

Neilson RP, King GA, Lenihan J (1994) Modeling forest response to climatic change: the potential for large emissions of carbon from dying forests. In: *Carbon balance of the world's ecosystems: Towards a global assessment* (ed. Kanninen M), pp. 150–162. Academy of Finland, Helsinki.

Neilson RP, Marks D (1994) A global perspective of regional vegetation and hydrologic sensitivities from climatic change. *Journal of Vegetation Science*, **5,** 715–730.

Neilson RP, Prentice IC, Smith B (1997) Annex C: Simulated changes in vegetation distribution under global warming. In: *IPCC: Special Report on Regional Climate Impacts. Contribution of the Intergovernmental Panel on Climate Change* (eds Watson RT, Zinyowera MC, Moss RH), pp. A1–A18. Cambridge University Press, Cambridge.

Neilson RP, Running SW (1996) Global dynamic vegetation modeling: couplingbiogeochemistry and biogeography models. In: *Global Change and Terrestrial Ecosystems* (eds Walker B, Steffen W), pp. 451–465. Cambridge University Press, Cambridge.

Overpeck JT, Rind D, Goldberg R (1990) Climate-induced changes in forest disturbance and vegetation. *Nature*, **343,** 51–53.

Pielke RA, Avissar R (1990) Influence of landscape structure on local and regional climate. *Landscape Ecology*, **4,** 133–156.

Schlesinger ME, Zhao ZC (1989) Seasonal climate changes induced by doubled CO_2 as simulated by the OSU atmospheric GCM-mixed layer ocean model. *Journal of Climate*, **2,** 459–495.

Sellers PJ, Bourdon L, Collatz GJ, Randall DA, Dazlich DA, Los SO, Berry JA, Fung I, Tucker CJ, Field CB, Jensen TG (1996) Comparison of radiative and physiological effects of doubled atmospheric CO_2 on climate. *Science*, **271**, 1402–1406.

Sellers PJ, Dickinson RE, Randall DA *et al.* (1997) Modeling exchanges of energy, water, and carbon between continents and the atmosphere. *Science*, **275,** 502–509.

Sellers PJ, Randall DA, Collatz GJ, Berry JA, Field CB, Dazlich DA, Zhang D (1995) A revised land surface parameterization (SiB2) for atmospheric GCMs. Part I: Model formulation. *Journal of Climate*, **9,** 676–705.

Seth A, Giorgi F, Dickinson RE (1994) Simulating fluxes from heterogeneous land surfaces: Explicit subgrid method employing the biosphere-atmosphere transfer scheme (BATS). *Journal of Geophysical Research*, **99** (D9), 18651–18667.

Smith TM, Shugart HH (1993) The transient response of terrestrial carbon storage to a perturbed climate. *Nature*, **361,** 523–526.

VEMAP Members (1995) Vegetation/ecosystem modeling and analysis project, Comparing biogeography and biogeochemistry models in a continental-scale study of terrestrial ecosystem responses to climate change and CO_2 doubling. *Global Biogeochemical Cycles*, **9,** 407–437.

Washington WM (1992) Climate-model responses to increased CO_2 and other greenhouse gases. In: *Climate System Modeling* (ed. Trenberth KE), pp. 643–668. Cambridge University Press, Cambridge.

Weeks ER, Tian Y, Urbach JS, Ide K, Swinney HL, Ghil M (1997) Transitions between blocked and zonal flows in a rotating annulus with topography. *Science*, **278,** 1598–1601.

Wendland WM, Bryson RA (1981) Northern hemisphere airstream regions. *Monthly Weather Review*, **109,** 255–270.

Wetherald RT, Manabe S, Cubasch U, Cess RD (1990) Processes and modeling. In: *Climate change: the IPCC scientific assessment* (eds Houghton JT, Jenkins GJ, Ephraums JJ), pp. 69–91. Cambridge University Press, New York.

Wilson CA, Mitchell JFB (1987) A doubled CO_2 climate sensitivity experiment with a global climate model including a simple ocean. *Journal of Geophysical Research*, **92** (D11), 13315–13343.

Woodward FI, Smith TM, Emmanuel WR (1995) A global land primary productivity and phytogeography model. *Global Biogeochemical Cycles*, **9,** 471–490.

Zeng N, Dickinson RE, Zeng X (1996) Climatic impact of Amazon deforestation – a mechanistic model study. *Journal of Climate*, **9,** 859–883.